Mode gaps in the refractive index properties of low-dose ion-implanted LiNbO3 waveguides

J. Rams, J. Olivares, P. J. Chandler, and P. D. Townsend

Citation: J. Appl. Phys. **87**, 3199 (2000); doi: 10.1063/1.372325
View online: http://dx.doi.org/10.1063/1.372325
View Table of Contents: http://jap.aip.org/resource/1/JAPIAU/v87/i7
Published by the American Institute of Physics.

Mode gaps in the refractive index properties of low-dose ion-implanted $LiNbO_3$ waveguides

J. Rams
ESCET, Universidad Rey Juan Carlos, C/Tulipán s/n, Móstoles 28933 Madrid, Spain

J. Olivares
Instituto de Óptica ''Daza de Valdés,'' CSIC, C/Serrano 121, 28006 Madrid, Spain

P. J. Chandler
Dazdaq Ltd, Acorn House, The Broyle, Ringmer, Sussex, BN8 5NW, United Kingdom

P. D. Townsend [a)]
School of Engineering, University of Sussex, Brighton BN1 9QH, United Kingdom

(Received 7 October 1999; accepted for publication 29 November 1999)

Data are presented for the refractive index profiles for low-dose He^+ ion-implanted $LiNbO_3$ waveguides. In the nuclear stopping region, the extraordinary index is increased for low ion doses, by contrast with index reduction normally associated with ion-implanted waveguiding structures. The index increase was confirmed by fabricating a buried waveguide for the extraordinary index by use of multi-energy implants. For single-energy implants, data are shown which map the extraordinary index at the surface together with that in the nuclear collision zone, as a function of angle relative to the *z* axis of light propagation in surface waveguides for *X* and *Y* cut $LiNbO_3$. These indices cross over near 45°, which results in a mode gap for which waveguide modes are not supported. A mechanism for this behavior is discussed based on defect-induced lattice relaxation. The phenomenon of a controlled mode gap may have applicability for optoelectronic and nonlinear materials and devices. © *2000 American Institute of Physics.* [S0003-6951(00)03104-1]

INTRODUCTION

$LiNbO_3$ is an outstanding material due to its high electro-optic and nonlinear optical coefficients and the fact that large single crystals are available at reasonable cost. Many of the applications require optical waveguides and an effective and competitive technique for guide fabrication in a wide range of optoelectronic and nonlinear materials is the use of ion implantation with light ions (He^+ or H^+). This is successful not only with $LiNbO_3$ but also in materials where chemical dopants to enhance the refractive indices are not available and implantation has become a practical route, with more than 50 examples reported so far.[1–4] Its general applicability comes from the simplicity of the physical mechanism that was proposed for defining a waveguide.[5,6] The original model capitalizes on the fact that the energetic light ions lose most of their initial kinetic energy, ~1 or 2 MeV, by electronic interaction within the first few microns of the sample, causing little or negligible structural damage. At the end of the ion track, the ions undergo elastic nuclear collisions, causing atomic displacements, which at high doses above a few times 10^{16}ions/cm^2 lead to partial or even complete amorphization of the lattice. Associated with this energy deposition and damage is a reduction of the density that is frequently accompanied by a decrease of refractive index. Such a decrease in index acts as a optical barrier and so defines a waveguide in the surface layer. The overall mechanism is insensitive to the target material but different insulator materials, although following this general model, show more specific features. In many cases the electronic energy deposition causes a small positive change of the extraordinary refractive index. Increases in index from nuclear collisions have been observed from bond compaction in some silicate glasses and in crystalline insulators index increases can occur from modified bond rearrangements (as in $Bi_4Ge_3O_{12}$[1,7]) or ionic motion ($LiNbO_3$).[1–4,8] At low ion beam doses ($\sim 1\times10^{16}$ions/cm^2) for crystals such as Nd:YAG there is a small increase in index.[1,9] With an expanding literature more subtleties in the shapes of the refractive index profiles have been noted, and many examples have been detailed in recent years for $LiNbO_3$, especially for the extraordinary index (n_e).[1,8,10] For example, it was found that the maximum increase of the extraordinary index is not at the surface, but is peaked deep inside the waveguide. This gives rise to the so called missing modes,[10] which are modes which cannot be coupled with a prism because they are buried (as indicated in current data). A further deeply buried strange mode, found for some limited implantation conditions, corresponds to an index enhancement beyond the damage barrier.[8] Nevertheless, in all the standard high dose cases, both n_o and n_e decreased by a few percentage in the nuclear damage region to provide the usual optical barrier. This was explained in terms of a decrease of density caused by the He^+ ion damage of the crystal. Explanations for the details of the n_e profile include diffusion of Li ions into the damage region, and/or lattice relaxation and restructuring.

For $LiNbO_3$ there have been no studies of the index profiles with small ion doses and in this letter we report on such

[a)]Electronic mail: p.d.townsend@sussex.ac.uk

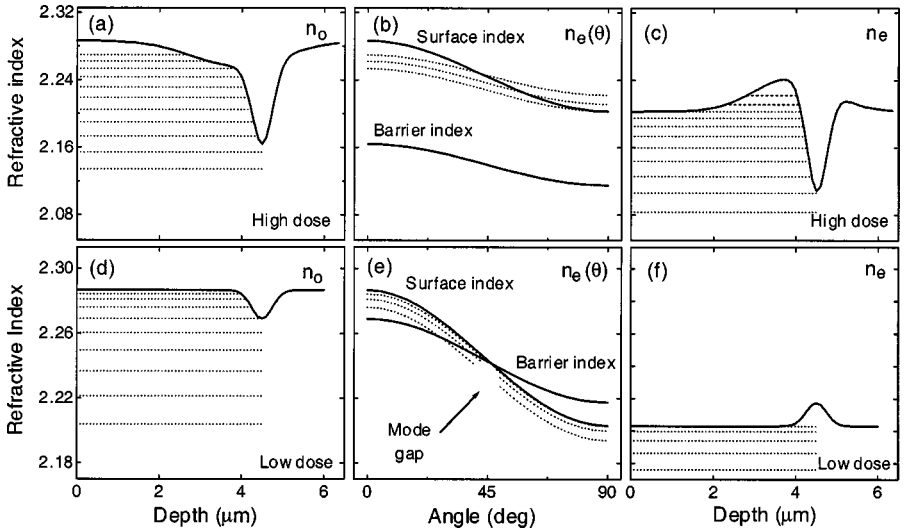

FIG. 1. Optical waveguide index profiles for He implanted guides in $LiNbO_3$. Results in (a), (b), and (c) are for high dose implantation (2×10^{16} ions/cm^2) and in (d), (e), and (f) are for low dose implantation (1×10^{15} ions/cm^2). Measured mode indices at $\lambda=0.633\,\mu$m are shown as horizontal dotted lines for the refractive indices of n_o ($\theta=0°$) and n_e ($\theta=90°$). The central figures, (b) and (e), show the angular dependence of the refractive indices, $n_e(\theta)$, between these extreme limits for the first three modes. Note, in the case of low dose implantation there is a mode gap around 45° 1(e), where modes are not detectable.

refractive index profiles, which differ considerably from the cases of high dose implantation with He ions. A novel feature of mapping the hybrid indices between n_o and n_e is the observation of a mode gap. New wave-guiding index structures resulting from multi-energy implants are also shown which give further support in the modelling of the unexpected refractive index behavior described here. A simple model is presented for the case of $LiNbO_3$ which could be relevant to other optoelectronic and nonlinear materials such as $KNbO_3$,[11–14] $BaTiO_3$,[14] $LiIO_3$,[15] etc, where ion implantation for waveguide formation is the only currently available route.

EXPERIMENTAL DETAILS

X and *Y*-cut $LiNbO_3$ samples were implanted with He^+ ions at 2.0 MeV energy at room temperature. Doses as low as 1×10^{15} ions/cm^2 were used (NB the standard dose for implanted waveguides in $LiNbO_3$ has been in the range $1-6\times10^{16}$ ions/cm^2). Three optical methods were used to determine the properties of the waveguides. Mode measurements leading to refractive index profiles were made with a dark mode reflectivity setup with a resolution better than 0.0001. Profiles were modelled via a fitting algorithm specifically developed for retrieving the index profiles of ion-implanted guides.[16] Although both transverse electric (TE) and transverse magnetic (TM) modes were routinely measured, only TE polarization is used for the study of the anisotropic behavior of the refractive index, i.e., for measuring the curve $n_{\mathrm{TE}}(\theta)$, θ being the angle between the light propagation direction and the optical *c* axis of the $LiNbO_3$ samples. By rotation of the *X*-or *Y*-cut samples under the coupling prism, keeping the light direction and the prism position fixed, the curve $n_{\mathrm{TE}}(\theta)$ for the confined modes and resonances above the isolation barrier were obtained. At the extreme points of the curve, the normal n_e and n_o indices are measured, for $\theta=90°$ and 0°, respectively. In the cases where there are buried modes which do not couple effectively to a surface prism, their presence can be inferred from the curve fitting and additionally their presence can be confirmed on going from $\theta=90°$ towards 0° as coupling will occur with changes in the index profile. Previous data[1,8,10] used several wavelengths and surface removal to confirm such examples of *strange* or *missing* buried modes.

Finally, with a standard end-coupling system with microscope objectives and a digitalized charge coupled device (CCD) camera, near field images of the out-coupled guided light were taken ($\theta=90°$), for TE and TM polarization, i.e. measuring extraordinary and ordinary modes, respectively. Choosing an input polarization at 45° to the sample surface, allows simultaneous coupling of TE and TM modes.

RESULTS

Figures 1(a) and 1(c), show the measured mode data and the resulting refractive index profile for the standard ion implantation dose (2×10^{16} ions/cm^2). The main point to note here is that in addition to the confined modes within the optical well of the waveguide the higher order resonances are still valuable in analysis of the form of the profile. Indeed, these extra data are essential for definition of complex profiles. Figures 1(b) and 1(e) contrast the measurements of the optical anisotropy study, $n_{\mathrm{TE}}(\theta)$, of the He implanted waveguides, for a low dose of 1×10^{15} ions/cm^2 (bottom row of figures) and for a standard high dose of 2×10^{16} ions/cm^2 (top row). The left hand [Figs. 1(a) and 1(d)] show the refractive index of modes and resonances (horizontal dotted lines) and the index profiles obtained from the mode analysis (solid line) for the ordinary refractive index $n_o(\theta=0°)$ for high and lose dose, respectively. Figures 1(c) and 1(f) show similar plots for the extraordinary refractive index $n_e(\theta=90°)$ for the high and low doses. Missing modes can be predicted, but surface coupling is inadequate to make measurements of them directly, nevertheless from earlier work their positions can be estimated, and an example occurs here where the two highest index modes in Fig. 1(c) are not accessible via surface prism coupling.

Of particular note is the n_e profile [Fig. 1(f)] which is determined for the low dose, as the index increases at the end of the ion range (i.e., as noted elsewhere for ion implanted Nd:YAG waveguides).[9] There is thus a divergence of behavior between n_o and n_e and in order to ascertain how the

transition between these extremes, observations were made for the hybrid modes by rotating the samples under the prism.

Figures 1(b) and 1(e) summarize the results and show there are smooth transitions in the refractive indices. In the case of the standard high dose waveguides [Fig. 1(b)], modes and resonances can be readily seen and measured for all angles. Their analysis is, however, far more difficult for this hybrid mode situation, hence the hybrid mode indices marked on Fig. 1(b) are less well determined than the precision values obtained at the end points of θ values of 0° and 90°. The data nevertheless confirm that a damage generated low index barrier exists for all values of θ. In the Fig. 1(b) we have only plotted the first three modes because their hybrid behavior is negligible. Higher order modes split in two different components because of the birefringent nature of $LiNbO_3$.[17] As shown by Fig. 1(b) there is also a smooth transition from n_o to n_e from easily coupled modes to predicted missing mode values. By contrast, on inspection of Fig. 1(e) for the small ion beam dose, there is a crossover in the values of the surface indices with those of the damage barrier. Consequently the measured modes become vanishingly faint when approaching an angle around $\theta = 45°$, resulting in a mode gap where modes can no longer be supported. This feature was initially unexpected, but in hindsight is consistent with the observations shown by Figs. 1(d) and 1(f). This is a novel result, which appears for doses up to $\sim 5 \times 10^{15}$ ions/cm^2, and it has been observed for any shape, size, and pressure of the optical contact.

Rigorously, for any intermediate angle, modes are no longer pure TE or TM, but they become hybrid modes, and any further detailed study should take this into account.[17] Nevertheless, for planar waveguides and for the highest effective index modes, as considered here, the hybrid character can be effectively neglected.

A similar pattern of modes and a mode gap, has been noted previously[18] in a study of double energy implanted $LiNbO_3$ waveguides for light propagating at different angles of θ. Their data show a similar mode gap, but in that work the authors did not offer any explanation for such behavior.

Although Fig. 1(f) indicates that a mode exists which has a higher index than the surface index it could not be supported within the very narrow region of raised index formed at the end of the ion track by nuclear collision damage. The possibility of confinement within a raised index region has been confirmed by building a wide high index zone using multi-energy implants. A low dose was used for several closely spaced ion energies. These multienergy He implants were made using energies of 2.00, 1.95, 1.90, 1.85, 1.80, 1.75, and 1.70 MeV, each with a dose of 1×10^{15} ions/cm^2. The n_e mode pattern of this structure differed strongly from the single energy case, where there was just one mode of slightly raised index. For the multi-energy case the effective modal indices are shifted to higher values, and the resonances through the barrier are mostly suppressed. The results are plotted in Fig. 2 for this multi-energy implanted guide. In Fig. 2(a) the dashed line represents the intensity distribution of the n_o guided light and the dotted line is that of the n_e light. There is one n_e missing mode, as

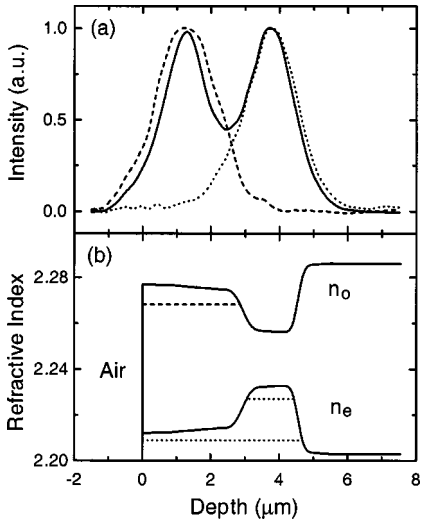

FIG. 2. Results obtained from a multi-energy implanted waveguide formed by using He+ energies of 2, 1.95, 1.9, 1.85, 1.8, 1.75, and 1.7 MeV, each with a dose of 1×10^{15} ions/cm^2. (a) Near field intensity profiles for the n_o values, as dashed line, and the n_e data are shown by a dotted one. The intensity profile for light polarized at 45° to the major axes of the sample surface is shown by the continuous line, (b) estimated refractive index depth profiles for this multi-energy implanted waveguide.

monitored from the surface prism, that exists within the raised index barrier zone, and so does not couple to the surface, but this was revealed by rotating the sample, as described previously.

In order to measure the depth and the width of the buried n_e waveguide, several near field images of the guided light were made with an end-coupling system. The polarization of the in-coupled light was changed from ordinary to extraordinary, without moving the relative positions of the sample, out-coupling objective or the CCD imaging camera. The near field intensity patterns are shown in Fig. 2(a). The double peaked solid line represents the profile measured for input light polarized at an angle of 45° to the surface sample, that is, when TE (n_e) and TM(n_o) modes are coupled simultaneously. When coupling was made only for n_o (ordinary light) the near field showed a waveguide at about 3 μm depth, extending from the surface, with a boundary defined by the reduced n_o index (the barrier). For n_e (extraordinary light) there are two different possibilities for waveguiding since two different types of mode can be excited. These are either a guided mode extending from the surface, to a depth of less than 4 μm, or a buried mode, of $\sim$1.5 μm width which commences some 2.5 μm from the surface. Figure 2 shows that most of the power is emitted in the near field pattern of the buried mode. Since ordinary polarized light is not guided in this buried barrier region there can be a spatial separation of the two polarizations in the near field patterns.

The results lead to the estimated index profiles shown in Figure 2(b). The multiple low dose implants with closely spaced energies generate a continuous extraordinary index increase at the end of the ion track that give rise to the buried mode. The accumulative electronic stopping effect (giving a slight increase of index from the surface throughout the ion range), that each implant generates, also allows a mode to be confined between the surface and a depth of almost 5 μm.

The near field intensity profiles described here imply that the propagation losses of the waveguides are low enough to transmit the guided light. Normally, for the standard high dose implanted waveguides the normal procedure requires a reduction of the losses in order to allow light transmission. Typically this is made via a low temperature annealing at 250 °C that removes absorbing color centers, but without making a significant change in the refractive index profile. Remarkably, for the low dose implanted waveguides we have found good light transmission, even before annealing. Nevertheless, transmission increases, as expected, with the annealing procedure. Further work is in progress to compare the final low loss values for the two cases, (i.e., from the standard dose and the low dose implanted guides).

Given that the waveguiding capabilities reported here are for the extraordinary polarization in the nuclear damage region, there is concern about its usefulness of the region for electro-optic and nonlinear devices. The restructuring of lattice involves some defects or deformed lattice, and these will reduce the relevant performance. However, this is offset by the access to the highest nonlinear coefficient of $LiNbO_3$ (d_{33}) which is addressed via the extraordinary polarization. A recent detailed study of the in depth profiles of the second order nonlinearity[19] showed that for implant doses lower than 5×10^{15} ions/cm^2, more that 50% of the value of the d_{33} bulk $LiNbO_3$ coefficient is still preserved. The value rises to 75% for the lower dose of 1×10^{15} ions/cm^2, even before annealing (i.e., which is a factor of 3 greater than available for n_o light). Further recovery of the nonlinearity is expected with annealing treatments, as for the case of high implant doses.

A simple explanation for the novel refractive index property can be given taking into account that $LiNbO_3$ is a material with a high negative birefringence, $\Delta n=0.08$, n_e being lower than n_o. In general, ion beam damage results in isolated point defects and ionic displacements, which at low doses allows some relaxation and distortion of the lattice. For a highly birefringent material this initially raises the lower index and decreases the larger one. Continued bombardment destroys the longer range lattice ordering and so can lead to total amorphization of a crystalline structure (e.g., as seen in the quartz to silica transitions where the two crystalline indices converge to a lower high density glass value).[1,2,20] In $LiNbO_3$ total amorphization appears not to be feasible since even for very high implant doses the ordinary and extraordinary indices never exactly match. Nevertheless, the pattern reported here, and in Ref. 18, is consistent with an n_e index increase from relaxation of a damaged lattice, followed by an overall decrease of both indices as pseudo-amorphization occurs to a lower density glassy structure.

CONCLUSIONS

The model is adequate to explain the effects but is rather simple and does not include more subtle contributions from changes in bond polarizability or stress induced distortions. The latter effects are well documented even in cubic and glassy materials, and so may contribute in the $LiNbO_3$. The same effect might exist in the isomorphous $LiTaO_3$, but as it has only a very small birefringence it may be difficult to observe; however, in other birefringent or biaxial materials, the lowest refractive indices could increase. Possible candidates are $CaCO_3$, KTP, BBO, LBO, KDP, or $KNbO_3$ and in the latter material such effects may be seen, although ''ultra low doses'' are required as the material damages more readily than $LiNbO_3$.[1,11,12]

The inherent presence of a mode gap, for many of these materials, in which light can only propagate over a limited angular range in a planar waveguide, opens the possibility of designing and engineering new types of surface waveguide devices.

ACKNOWLEDGMENTS

The authors thank B. W. Farmery for the implants and one of the authors (J.O.) acknowledges a Marie Curie grant.

[1] P. D. Townsend, P. J. Chandler, and L. Zhang, *Optical Effects of Ion Implantation* (Cambridge University Press, Cambridge, 1994).
[2] P. J. Chandler, L. Zhang, and P. D. Townsend, Solid State Phenom. **27**, 129 (1992).
[3] Ch. Buchal, S. P. Withrow, C. W. White, and D. B. Poker, Annu. Rev. Mater. Sci. **24**, 125 (1994).
[4] P. D. Townsend, Nucl. Instrum. Methods Phys. Res. B **89**, 270 (1994).
[5] P. D. Townsend, Inst. Phys. Conf. Ser. **28**, 104 (1976).
[6] G. L. Destefanis, P. D. Townsend, and J. P. Gailliard, Appl. Phys. Lett. **32**, 293 (1978).
[7] S. M. Mahdavi and P. D. Townsend, Nucl. Instrum. Methods Phys. Res. B **65**, 251 (1992).
[8] L. Zhang, P. J. Chandler, and P. D. Townsend, J. Appl. Phys. **70**, 1185 (1991).
[9] L. Zhang, P. J. Chandler, P. D. Townsend, S. J. Field, D. C. Hanna, D. P. Shepherd, and A. C. Tropper, J. Appl. Phys. **69**, 3440 (1991).
[10] P. J. Chandler, L. Zhang, J. M. Cabrera, and P. D. Townsend, Appl. Phys. Lett. **54**, 1287 (1989).
[11] F. P. Strohkendl, D. Fluck, P. Günter, R. Irmscher, and Ch. Buchal, Appl. Phys. Lett. **59**, 3354 (1991).
[12] T. Pliska, C. Solcia, D. Fluck, P. Gunter, L. Beckers, and C. Buchal, J. Appl. Phys. **81**, 1099 (1997).
[13] P. Bindner, A. Boudrioua, P. Moretti, and J. C. Loulergue, Nucl. Instrum. Methods Phys. Res. B **142**, 329 (1998).
[14] P. Moretti, P. Thevenard, K. Wirl, P. Hertel, H. Hesse, E. Kratzig, and G. Godefroy, Ferroelectrics **128**, 13 (1992).
[15] C. Rosso, P. Moretti, J. Mugnier, D. Barbier, Y. Teisseyre, and J. Bouillot, Phys. Status Solidi A **139**, K137 (1993).
[16] P. J. Chandler and F. Lama, Opt. Acta **33**, 127 (1986).
[17] A. Knoesen, T. K. Taylor, and M. G. Moharam, J. Lightwave Technol. **6**, 1083 (1989).
[18] S. S. Sarkisov, E. K. Williams, D. Ila, P. Venkateswarlu, and D. B. Poker, Appl. Phys. Lett. **68**, 2329 (1996).
[19] J. Rams, J. Olivares, P. J. Chandler, and P. D. Townsend, J. Appl. Phys. **84**, 5180 (1998).
[20] P. J. Chandler, L. Zhang, and P. D. Townsend, Nucl. Instrum. Methods Phys. Res. B **46**, 69 (1990).